Lidar Analyses

Contract No. NAS8-38609

Delivery Order No. 79

Contract Period 7/01/93 - 10/30/94
Report Date 9/18/95

Gary D. Spiers
Center for Applied Optics
University of Alabama in Huntsville
Huntsville
AL 35899
(205) 895 6030 ext. 420

Table of Contents

Introduction

This report details work carried out under NASA contract NAS8-38609 delivery order no. 79.

A brief description of enhancements made to the NASA MSFC coherent lidar model is provided. Notable improvements are the addition of routines to automatically determine the 3 dB misalignment loss angle and the backscatter value at which the probability of a good estimate (for a maximum liklihood estimator) falls to 50%. The ability to automatically generate energy/aperture parameterisation (EAP) plots which include the effects of angular misalignment has been added. These EAP plots make it very easy to see that for any practical system where there is some degree of misalignment then there is an optimum telescope diameter for which the laser pulse energy required to achieve a particular sensitivity is minimised. Increasing the telescope diameter above this diameter will result in a reduction of sensitivity. These parameterisations also clearly show that the alignment tolerances at shorter wavelengths are much stricter than those at longer wavelengths.

A brief outline of the NASA MSFC AEOLUS program is given and a summary of the lidar designs considered during the program is presented. A discussion of some of the design trades is performed both in the text and in a conference publication attached as an Appendix.

1.0 Improvements to the Lidar Model

The following improvements have been made to the NASA MSFC coherent lidar model [1].

1.1 Back solution of misalignment angle required for 3dB loss

In order to assess the alignment tolerance of different lidar point designs, it is convenient to look at the misalignment angle required to give a 3 dB SNR loss. Code to automatically determine the misalignment angle required to achieve a 3 dB misalignment loss was added to the existing model and a button added to the tool bar to enable easy user access to this function. This means that the user can now change the telescope diameter and then have the program calculate the corresponding 3 dB misalignment angle from any where within the model. The angle is calculated by back solving from the required solution to determine the input variable. The code is listed in Appendix (Ia).

1.2 Back solution of backscatter required for 50% probability

At low SNR values the velocity estimation algorithms may incorrectly identify a noise spike as the signal returned from the atmosphere. The probability that such an event will occur is directly related to the sensitivity of the instrument. The coherent lidar community has adopted the value of backscatter at which this probability is 50% (i.e. 50% of the time the estimator correctly estimates the wind velocity) as a measure of the sensitivity of a coherent lidar system and all the AEOLUS designs discussed in this report use this as a sensitivity comparison point. Code was developed so that when a new instrument design has been entered into the model a toolbar button can be used to initiate an automated back-solution to find the backscatter value required to achieve this sensitivity value. The code is listed in Appendix (Ib).

1.3 Energy-aperture design trades code

The energy-aperture product (EAP) has traditionally been used as a figure of merit for a lidar design and plots of pulse energy vs. telescope diameter for constant atmospheric backscatter have been used to determine design points for coherent lidars [2]. Such plots assume perfect alignment of the optical system and for a fixed pulse energy show continuous improvement in sensitivity as the telescope diameter is increased. Unfortunately in any practical system, particularly those involving rotating optical components such as the scanning system employed in coherent lidars, there is the potential for an angular misalignment to occur between the received beam (signal) and the local oscillator (lo) beam. Any angular misalignment in the system between the signal and lo beams results in a loss of mixing efficiency [3] and reduces the sensitivity of the instrument. The lidar model was enhanced by developing code (Appendix (Ic)) to plot the EAP as a function of misalignment angle for a fixed sensitivity (backscatter) or as a function of varying sensitivity with a fixed misalignment angle . Figure (1.1) shows EAP plots for both 2 μm and 9 μm lidars in which the misalignment angle has been allowed to vary whilst the 50% probability (Section 1.2) for each wavelength was held constant at the value indicated. Figure (1.2) shows a similar plot for both the 2 μm and 9 μm wavelengths when the misalignment angle is held constant at the value required for a 3 dB loss with a 0.5 m diameter telescope and the sensitivity is allowed to vary.Table (1.1) lists the model parameters used to generate the plots.

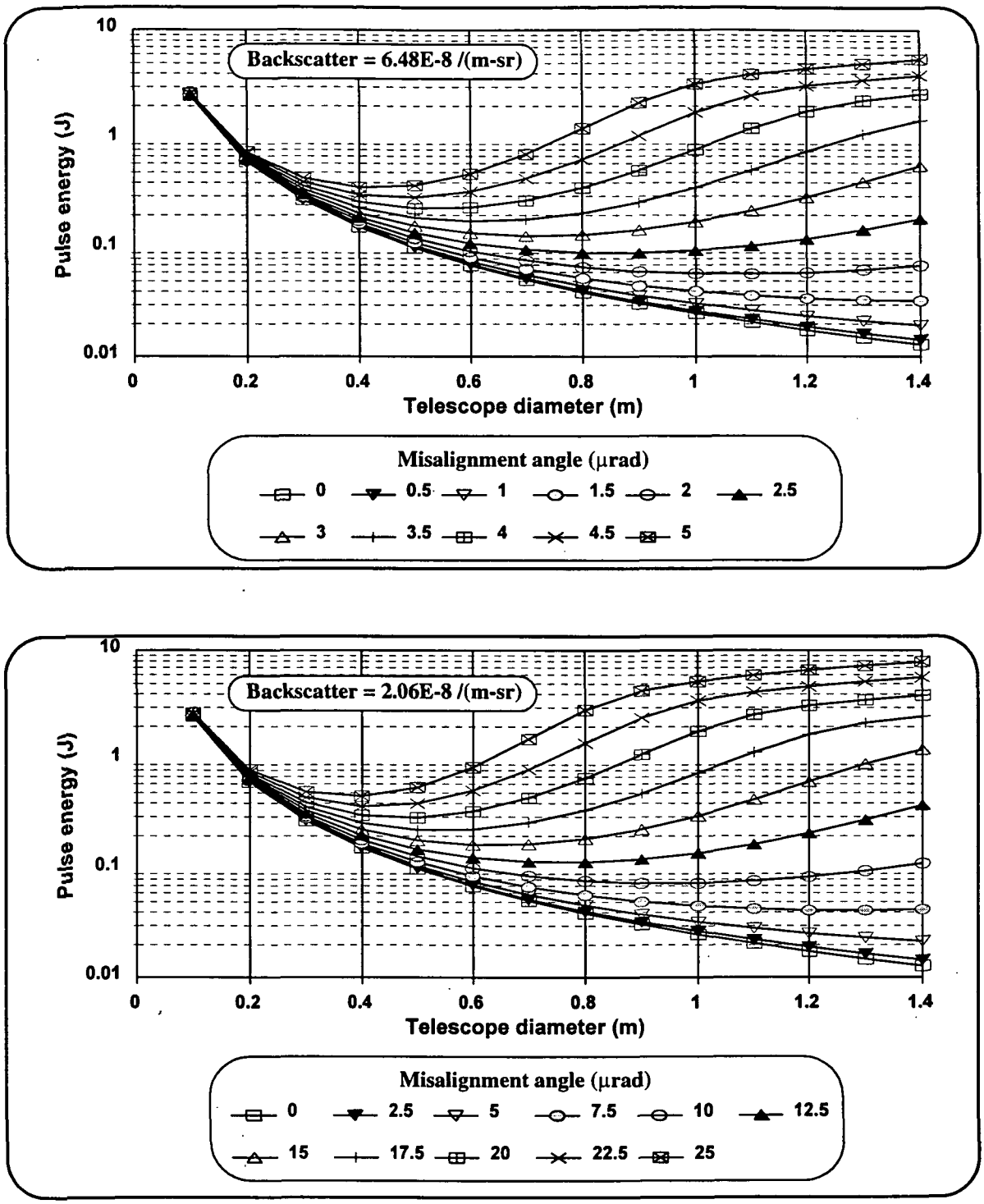

Figure (1.1) EAP plots for a 2 μm (top) and a 9 μm (bottom) lidar as a function of misalignment angle for a fixed sensitivity (see text).

It can be seen that the misalignment sensitivity of the 2 μm system is much greater than for the 9 μm system. It is easy to understand this by considering that the heterodyne mixing is dependent on the signal and local oscillator overlap function [3]. As the angular misalignment between the local oscillator and signal beam increases the degree of overlap also decreases. For a given tele-

Parameter	Value	Parameter	Value
Orbit height	350 km	Receiver type	Complex
Orbit inclination	98 deg.	Receiver geometry	Wang
Laser wavelength	2.065479 μm 9.1145187 μm	Detector quantum efficiency	0.6 for 2 μm 0.4 for 9 μm
Laser pulse energy	See plots	Scan mechanism	Wedge
Laser pulse length	0.5 μs	System margin	0.5
Laser P.R.F.	10 Hz	Atmospheric model	Midlatitude summer clear
Telescope diameter	see plots	Target aerosol altitude	1 km
Nadir angle	30 deg.	Processing bandwidth	± 20 m/s
Transmit optics transmission	0.9	Receive optics transmission	0.9
Polarisation efficiency	1	Misalignment angle	see plots

Table (1.1) Parameters used for EAP plots.

scope size the diameter of a diffraction limited beam at 2 μm, after propagation through a large distance, will be smaller than that for a 9 μm beam. Thus the overlap between the signal and local oscillator beams will decrease more rapidly at the shorter wavelength.

It can also be seen that for a given misalignment angle there is an optimum telescope diameter at which the laser pulse energy required to achieve a particular sensitivity is minimised. This is very important for the design of a space-based lidar as the delay between output pulse transmission and signal return can be several milliseconds. If there is jitter in the spacecraft pointing during this round trip period it will be equivalent to an angular misalignment of the optical system such that even a perfectly aligned optical system will be unable to reap the benefits of a large telescope diameter. Thus the spacecraft jitter, rather than tolerances in the optical design, may be the dominant mechanism limiting the choice of telescope diameter. Given the small misalignment (3.64 μrad) required for a 3 dB loss at 2 μm for a 0.5 m telescope and the generally ill--defined stability specifications of many small spacecraft any design placing a short wavelength coherent lidar on a small spacecraft must be fully aware of this potential problem.

1.4 Other Improvements

A number of small improvements were made to the model. These included expanding the lookup table for the maximum liklihood estimator to cover a wider range of values of Omega and M, changing the misalignment loss vs. angle plot to an alignment efficiency vs. angle plot (more intuitive this way), moving the "update performance" plots button to the toolbar so that it is accessible from everywhere, adding a few additional calculated fields and several other minor changes.

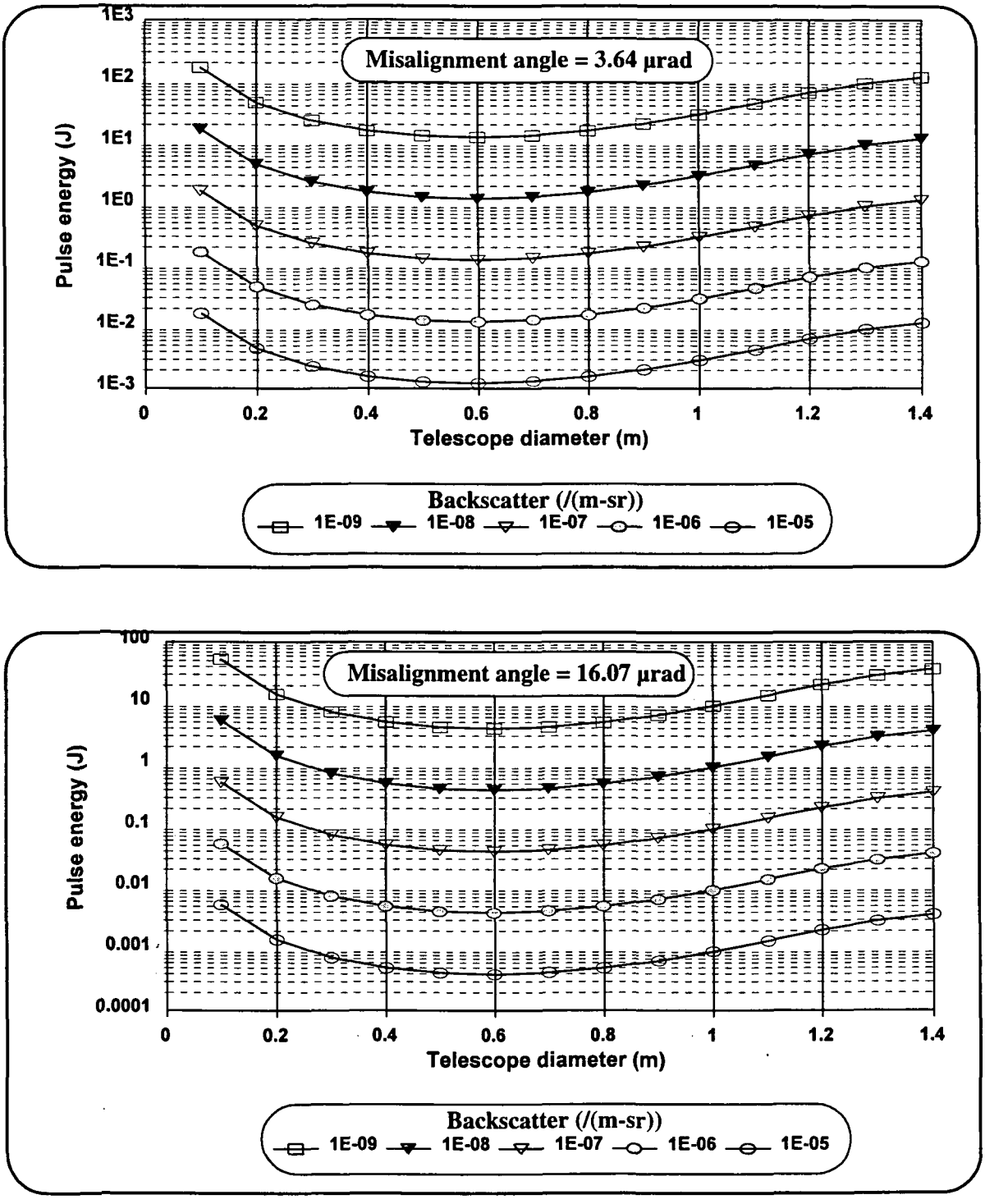

Figure (1.2) EAP plots for a 2 µm (top) and a 9 µm (bottom) lidar as a function of backscatter for a fixed misalignment angle (see text).

1.5 References

[1] Gary D. Spiers, "Lidar Performance Analysis", Final Report on NASA Contract No. NAS8-38609, Delivery Order 57.

[2] See for example Figure 3-21 on page 3-18 of Lockheed Missiles & Space Company, "Phase II Design Definition of the Laser Atmospheric Wind Sounder (LAWS)", DR-20 Vol. II: Final Report, Nov. 1992, Prepared for NASA George C. Marshall Space Flight Center, AL 35812 under NASA contract NAS8-37590. and also page 198 of TRW Applied Technology Division, "LAWS Laser Atmospheric Wind Sounder Two-Micron LAWS System Study", Final Report, October 1993, under contract NAS1-19291 MSOA, Task 13.

[3] Rod G. Frehlich, "Heterodyne efficiency for a coherent laser radar with diffuse or aerosol targets", J. Mod. Optics, 41, 11, 2115-2129 (1994).

2.0 AEOLUS

AEOLUS is an acronym for Autonomous Earth Observing Lidar Utility Sensor and is a series of studies carried out at the NASA Marshall Space Flight Center towards developing a small space-based coherent lidar. A fairly complete description of AEOLUS and some of the design issues involved were presented in the paper "Direct global measurements of tropospheric winds employing a simplified coherent laser radar using fully scalable technology and technique" presented at SPIE's International Symposium on Optical Engineering in Aerospace Sensing, Technical Conference 2214 on Space Instrumentation and Dual-Use Technologies, session on "Faster, Cheaper, Smaller Space Science Optical Instruments," Orlando, FL (6 April 1994). This paper is included here as Appendix II and is the main source of information concerning the AEOLUS designs.

2.1 Description of the AEOLUS Designs

The following tables summarises all of the AEOLUS designs analysed.

	Scenario					
Parameter	**1**	**2**	**3**	**4**	**5**	**Units**
Wavelength, λ	9.11	9.11	2.065	2.065	2.065	μm
Pulse energy, E	400	400	200	200	25	mJ
Pulse length, τ	0.5	0.5	0.2	0.2	0.5	μs
Max. pulse rate, PRF	20	20	10	10	50	Hz
Detector Q.E.	0.4	0.4	0.6	0.6	0.6	
Telescope diameter, D	0.5	0.5	0.5	0.5	0.25	m
Scanning method	Line scan	Wedge	Line scan	Wedge	Wedge	

	Scenario					
Parameter	**6**	**7**	**8**			**Units**
Wavelength, λ	2.065	2.065	2.065			μm
Pulse energy, E	25	25	200			mJ
Pulse length, τ	0.5	0.5	0.2			μs
Max. pulse rate, PRF	15	15	10			Hz
Detector Q.E.	0.6	0.6	0.6			
Telescope diameter, D	0.25	0.233	0.5			m
Scanning method	Wedge	Wedge	Wedge			

Table (2.1) The AEOLUS configurations considered.

Designs 1-4 were the initial point designs in which both 9 μm and 2 μm lidar systems were considered. It was felt that the large rotating telescope used in the original LAWS concepts was too unwieldy for a small satellite design and so two alternate scan geometries were developed. The first used a pair of telescopes to point fore and aft to one side of the satellite (designs 1 & 3) - this produces a single line scan sampling pattern[1]. The two telescopes share a common volume and a common secondary mirror. The second concept uses a refractive wedge mounted in front of a nadir pointing telescope to produce a conical scan (designs 2 & 4)[1].

The dual-telescope approach was discarded because of limited coverage and awkward packaging and the 2 μm wedge scanned lidar (design 4) was favoured over the 9 μm equivalent (design 2)

because the need to cool the 9 μm detector introduced an additional power drain and thermal heat source (mechanical cooler) which has the potential to introduce vibration into the optical system. The 2 μm design also held the potential for the laser to be smaller and more compact than the 9 μm equivalent. It should be noted that the pulse energies for the 2 μm and 9 μm designs listed in Table (2.1) were based on likely availability of a suitable laser from a vendor rather than from any lidar sensitivity issues and so they should not be assumed to be of equivalent performance.

Design 5 attempted to develop a lidar small enough to fit on a Pegasus class launch vehicle. The limited sensitivity of such a small instrument indicated that most of the useful signal returns would probably be obtained from clouds. Therefore two backscatter values were determined for this instrument, one for a 1 km thick diffuse target (thin clouds or high aerosol concentration boundary layer) and one for a pulse width limited target (thick clouds). The instrument was designed to operate at a high PRF (50 Hz) to give a good shot pattern density and provide good statistical sampling of the atmosphere. Spacecraft accomodations at NASA MSFC determined that a combination of power and weight limitations aboard likely spacecraft limited operation of the instrument to ~ 30 % of each orbit. Discussions with the former LAWS Science Team indicated that they would prefer a greater orbit coverage and lower shot density. This led to design 6 which is identical to design 5 with the exception of the PRF and orbit duty cycle, however the total number of shots per orbit remained the same.

One consequence of operating the lidar over a whole orbit (design 6) was that ancillary equipment such as the receiver electronics also had to remain powered on. When this was factored in to the power budget the spacecraft accomodations people at NASA MSFC felt that the power budget was too high and so a design trade was carried out to arrive at design 7.

Finally design 4 was revisited and the orbit duty cycle increased to 100 % in accordance with the preferences of the former LAWS Science Team. This resulted in two designs, one for a smallsat (design 7), Pegasus class launch and one (design 8) for a larger (but still small c.f. LAWS) instrument.

2.2 Instrument Performance

The basic parameter used to characterize the sensitivity of each design was the value of backscatter at which the probability of correct detection of the return signal from the atmosphere was 50%. This was calculated using the lidar model outlined previously[1]& Section 1.0. Table (2.2) and Table (2.3) list the common parameters used for the analysis..whilst Table (2.4) summarises the

Orbit height	350	km	Receiver type	Complex	
Orbit inclination	98	deg	Receiver geometry	Wang	
Nadir angle	30	deg	Target altitude	1000	m
Transmit optics efficiency	0.9		Horizontal wind velocity processing search space	± 20	m/s
Receive optics efficiency	0.9		Vertical range integration (Clear Air)	1000	m
			(Clouds)	63.67	m
Polarisation efficiency	1		Mid-latitude summer -clear atmosphere		

Table (2.2) Parameters common to all scenarios.

System margin	0.5		WPL-37 refractive index structure constant profile

Table (2.2) Parameters common to all scenarios.

	Scenario						
	1	2	3	4 & 8	5 & 6	7	Units
Effective telescope diameter, D_{eff}	0.5	0.433	0.5	0.433	0.217	0.202	m
BPLO/signal misalignment angle, α	13.91	16.07	3.15	3.64	7.28	7.81	μrad

Table (2.3) Effective telescope diameter and misalignment angle tolerance for each of the five scenarios assuming a nadir angle, θ_n of 30 degrees.

	Design No.					
	1	2	3	4 & 8	5 & 6	5b & 6b
β(50%) (/(m-sr))						
@ 1 km vert. resoln.	7.7×10^{-9}	1.0×10^{-8}	4.8×10^{-8}	6.4×10^{-8}	2.1×10^{-6}	2.4×10^{-5}
@ 64 m vert. resoln.					2.3×10^{-5}	2.6×10^{-5}

Table (2.4) AEOLUS backscatter values for a 50% probability of correct detection.

sensitivity obtained from each system.

2.3 Mass and Power Trade on Design 6.

As was mentioned earlier, the AEOLUS design no.6 was found to be too power hungry (for a Pegasus class launch) by the spacecraft accommodations people. They provided an estimate that for every Kg of mass given up by the instrument, approximately 20 W of power could be gained from the spacecraft by increasing the solar array size.

For the initial instrument design, the spacecraft could supply 200 W of power, which was insufficient for the instrument, however it was realised that by reducing the diameter of the Ge wedge scanner, the weight of the instrument could be reduced thereby freeing up mass for the power system. Figure (2.1) shows the wedge mass as a function of its diameter. It can be seen that large weight savings can be obtained for small changes in the wedge diameter. Figure (2.2) shows the laser and instrument power as a function of laser pulse repetition frequency (PRF). Also plotted is the wedge optical diameter as a function of the laser PRF.

For laser PRFs below 5 Hz the instrument power is less than 200 W and no weight reduction is needed, however above 5 Hz the power required is greater than 200 W and the instrument mass needs to be reduced to increase the size of the spacecraft power system. Thus above 5 Hz PRF the optical diameter of the wedge reduces. It has been suggested (Dr. G.D. Emmitt - private communication) that for optimum sampling of the atmosphere with this instrument, a laser PRF of ~10 - 20 Hz would be advantageous. It can be seen that at a PRF of 15 Hz, the instrument requires ~230 W. This power can be achieved by reducing the wedge optical diameter to 24.3 cm from the original 25 cm diameter. This results in a small 0.7 dB loss in SNR. Thus by trading weight for power the instrument design has been improved. It should be noted that this is a conservative trade, as neither the telescope primary mirror nor the support structure have been reduced .

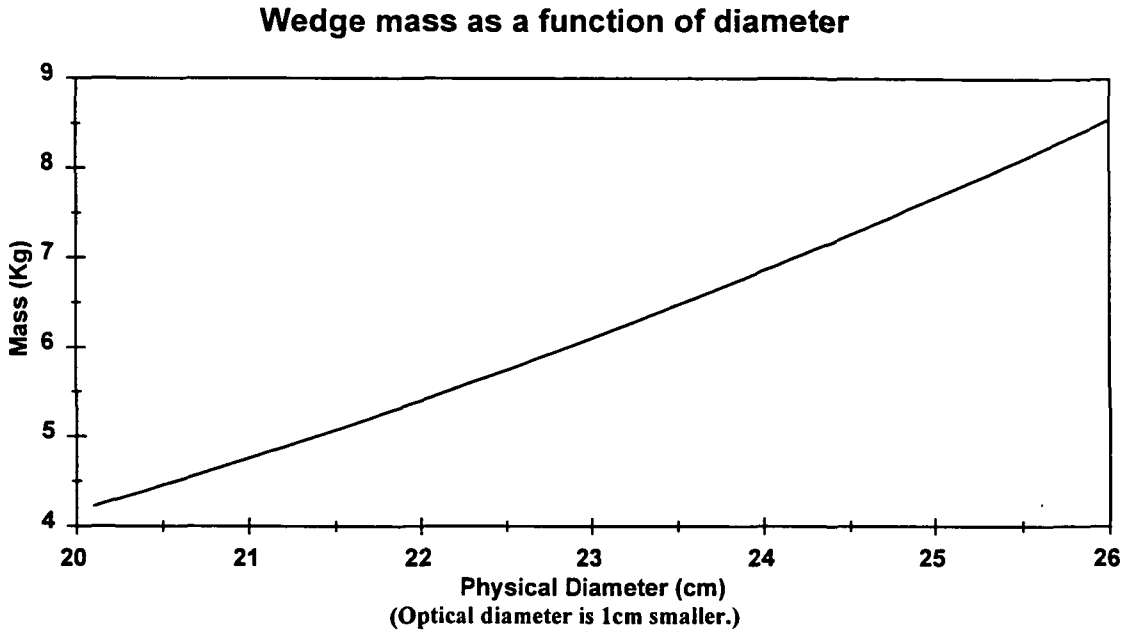

Figure (2.1) Dependence of wedge mass on diameter

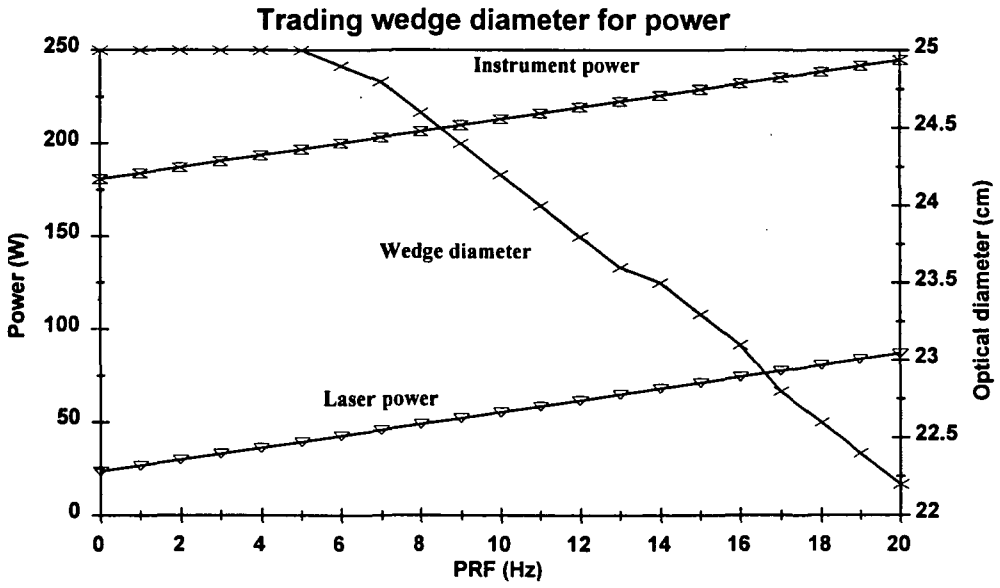

Figure (2.2) Trading wedge diameter for increased power to the instrument.

Appendix I Lidar Model Code

The code listed here follows the same conventions as listed in the previous report[1]. The code makes use of the OPTIMIZER routine built into Quattro Pro and it has been found that this routine is very reliable when solving for a value if the initial guess is less than the final value. When the guess value is larger than the final value the routine will occasionally fail to find a solution - thus each use of the OPTIMIZER explicitly sets the initial guess value for the unknown to a value much smaller than any solution likely to be encountered.

Appendix (Ia) Code to calculate 3dB misalignment angle

The following table is a coded macro to backsolve for the misalignment angle required to give a 3 dB SNR loss. It is executed when the user clicks on the "3dB Loss" button on the toolbar.

	A	B	C
37	THIS MACRO CALCULATES THE BPLO/SIGNAL MISALIGNMENT ANGLE REQUIRED FOR A 3dB LOSS		
38			
39			
40			
41	3dB_angle	18.20474	
42	Current_angle	7.81320	
43	Current_loss_dB	14.37397	
44			
45			
46			
47	3dB_calc	{LET $Current_angle, @ROUND($Align_angle,6)}	Store current angle
48		{LET $Current_loss_dB, @ROUND(-10*@LOG($eta_misalign),6)}	Store current misalignment angle
49		{Optimizer.Reset}{Optimizer.Solution_cell [lidar]$eta_misalign}	Set OPTIMIZER to solve for misalignment efficiency
50		{Optimizer.Solution_goal Target Value}	OPTIMIZER to aim for a target value
51		{Optimizer.Target_Value 0.5}	Set target value
52		{Optimizer.Variable_cells [lidar]$Align_angle}	Vary misalignment angle
53		{Optimizer.Add 1,"Align_angle",>=,"0"}	Keep misalignment angle >=0
54		{Optimizer.Solve}	Solve!
56			

Appendix (Ib) Code to calculate β(50%)

This table contains macro code which is used to backsolve for the backscatter value at which the probability of a good estimate is equal to 50%. It is executed when the user clicks on the "β(50%) button on the toolbar."

	A	B	C
62			
63	THIS MACRO CALCULATES THE BACKSCATTER REQUIRED TO GIVE A 50% PROBABILITY		
64	OF A GOOD ESTIMATE AND INSERTS THIS BACKSCATTER VALUE INTO THE MODEL.		
65			
66			
67	50%BETA_CALC	{LET $Save_beta, $beta}	Save existing value of backscatter (the save_beta variable is with the performance calculation macro)
68		{LET $beta,1e-13}	Set the initial guess for beta to a very small value.
69		{Optimizer.Reset}{Optimizer.Solution_cell [lidar]$Pgood}	Set OPTIMIZER to solve for Pgood.
70		{Optimizer.Solution_goal Target Value}	Set OPTIMIZER to solve for a target value of Pgood.
71		{Optimizer.Target_Value 0.5}	Set target value of Pgood as 0.5.
72		{Optimizer.Variable_cells [lidar]$Beta}	Tell OPTIMIZER to vary backscatter to achieve target value.
73		{Optimizer.Solve}	Solve!

Appendix (Ic) Code to calculate and display an EAP plot

This macro is executed when the user clicks on the EAP button on the toolbar. When run it moves to a screen displaying a photograph of hurricane Gladys. This is purely for aesthetic reasons and provides the user with something to look at while the code is run as this can take some time if a large parameter space is selected. A dialog box is then displayed giving the user a choice of two types of EAP plot as discussed previously(Section 1.3). After a selection has been made another dialog box is then displayed to allow the user to enter the minimum and maximum values required for each of the independent variables and the number of intermediate steps between these extrema. The telescope diameter is treated as an independent variable for both types of EAP plot whilst the misalignment angle and backscatter alternate as the second independent variable according to the plot type selected by the user. When backscatter is an independent variable the intermediate values are calculated for a log axis whilst a linear scale is used for intermediate values of misalignment angle. The value of the fixed parameter is taken from the current value in the model and the routine then solves for the pulse energy required to achieve Pgood = 50% for each combination of telescope diameter, backscatter and misalignment angle. When all the values are computed the routine edits the EAP plot, changing the series and updating axis labels and scalings as necessary to provide a reasonable plot..The plot is then displayed to the user.

	A	B	C
76	THIS MACRO CALCULATES AND DISPLAYS AN EAP PLOT AND ALLOWS THE USER TO CHOOSE		
77	BETWEEN CONTOURS OF CONSTANT BACKSCATTER OR MISALIGNMENT ANGLE.		
Rows 78 - 84 are all blank and have been skipped in this table.			
85	eap_option	0	Used to determine type of EAP plot required: 1 = vary misalignment angle 0 = vary backscatter
86	save_angle	16.0667307422832	
87	save_tscope	0.5	
88	save_energy	0.2	
89	tscope_min	0.1	
90	tscope_max	1.5	
91	tscope_nstep	14	
92	eapvar_min	1E-09	eapvar is either misalignment angle or backscatter
93	eapvar_max	1E-05	
94	eapvar_nstep	4	
95	loop1_count	6	Counter for tscope diameter
96	loop2_count	5	Counter for angle or backscatter
97	row_number	32	Used to locate position in results table.
98	col_number	80	Used to locate position in results table.
99	tscope_step	($TSCOPE_MAX-$TSCOPE_MIN)/ $TSCOPE_NSTEP	Calculates incremental step to evenly space telescope diameter values on x-axis.
100	eapvar_step	($EAPVAR_MAX-$EAPVAR_MIN)/ $EAPVAR_NSTEP	Calculates incremental step for misalign-ment angle only NOT backscatter.

	A	B	C
101	a	@LOG($EAPVAR_MIN)	a and bval are used to uniformly distribute backscatter values alnog a logarithmic scale.
102	bval	(@LOG($EAPVAR_MAX)-$A)/ ($EAPVAR_NSTEP)	
103	marker_style	@IF(LOOP1_COUNT>9,+"M"&@STRING($LOOP1_COUNT,0)&",5,0",+"M0"&@STRING($LOOP1_COUNT,0)&",5,0")	This expression constructs a marker style tag so that each data series has a unique symbol.
104	guess	1E-06	Used to set up OPTIMIZER
105	old_nstep	4	Used to clear old results table.
106			
107	loop1_calc	{EditGoto [lidar]EAP:A1}{LET guess,1e-6}{LET $save_beta, $beta}	Goto the existing EAP plot (allways exists), set the OPTIMIZER guess value to a small value and save the current value of the backscatter.
108		{LET $save_tscope,$tscope_d}{LET $save_angle,$align_angle}	Save exisiting values of the telescope diameter and misalignment angle.
109		{LET $save_energy, $nrg}{WindowsOff}	Save existing laser pulse energy and turn screen updates off during macro execution.
110		{EditGoto Cover:A1}{DODIALOG EAPoptions,dialog_ans,eap_option}{IF dialog_ans=0}{RETURN}	Goto a pretty picture! Then display the dialog box offering a choice of eap plots. Choice is stored in eap_option as a 0 or 1. if user cancels this dialog quit.
111		{IF eap_option=1}{setup_varyangle}	If user chose fixed backscatter and varying angle jump to a routine to setup that calculation.
112		{IF eap_option=0}{setup_varybeta}	If user chose fixed angle and varying backscatter jump to setup routine for that option.
113		{EditGoto Cover:A1}{DODIALOG loopprops,dialog_ans,loop_vars}{IF dialog_ans=0}{RETURN}	Display the input parameter dialog box so the user can enter values. If they cancel the dialog then quit.

	A	B	C
114		{SELECTBLOCK +"EAP:A31..EAP:"&@CHAR(col_number)&@STRING(row_number+old_nstep,0)}{DEL}	This deletes the results table from the previous EAP plot.
115		{calc}{LET col_number,@CODE("B")}{LET row_number,32}	This resets column and row tracking cells used to build results table.
116		{FOR loop1_count, tscope_min,tscope_max,tscope_step, loop2_calc}	Loop over the telescope values.
117		{GraphEdit EAP}{GraphSettings.Type "XY,2-D"}	Finished calculating results so edit EAP plot to display results.
118		{Series.Data_Range "XAxisLabelSeries", +"EAP:B31..EAP:"&@CHAR(col_number-1)&"31",1}	Set up the x-axis range (telescope diameter).
119		{Series.Data_Range "LegendSeries",+"EAP:A32..EAP:A"&@STRING(row_number+eapvar_nstep,0),1}	Set up the values for the legends (either misalignment angle or beta)
120		{FOR loop1_count,1,eapvar_nstep+1,1,series_fill}	For each value of misalignment angle or beta generate fill a series with data as a fn. of tscope diameter.
121		{Series.Go}{WindowClose}	Carry out graph changes and close the graph edit window.
122		{FOR loop1_count,1,eapvar_nstep+1,1,series_chng}	Run a routine to edit each of the data series.
123		{SETOBJECTPROPERTY "EAP:G$Y1Axis.Major_Grid_Style","S5W1,0,0,0"}	Set up Y-axis grid style.
124		{SETOBJECTPROPERTY "EAP:G$Y1Axis.Text_Font","Arial,10,Yes,No,No,No"}	Set up font for Yaxis labels.
125		{SETOBJECTPROPERTY "EAP:G$X1Axis.Text_Font","Arial,10,Yes,No,No,No"}	Set up font for Xaxis labels.

	A	B	C
126		{SETOBJECTPROPERTY "EAP:G$Leg-end.Text_Font","Arial,10,Yes,No,No,No" }	Set up font for series legends.
127		{SETOBJECTPROPERTY "EAP:G$Y1Title.Text_Font","Arial,12,Yes,No,No,No"}	Set up Yaxis title font.
128		{SETOBJECTPROPERTY "EAP:G$X1Title.Text_Font","Arial,12,Yes,No,No,No"}	Set up Xaxis title font.
129		{IF eap_option=1}{GraphSettings.Titles "EAP plot, constant backscatter value","solved for energy to give Pgood=0.5.",Telescope diameter (m),Pulse energy (J),""}	If varying misalignment angle then change graph title and axis labels to match option chosen.
130		{IF eap_option=0}{GraphSettings.Titles "EAP plot, constant misalignment angle","solved for energy to give Pgood=0.5.",Telescope diameter (m),Pulse energy (J),""}	If varying backscatter then change graph title and axis labels to match option chosen.
131		{LET $tscope_d, $save_tscope}{LET $beta,$save_beta}	Restore telescope diameter and backscatter to their original values.
132		{LET $nrg,$save_energy}{LET $align_angle,$save_angle}	Restore energy and misalignment angles to their original values.
133		{LET old_nstep,eapvar_nstep}	Save value of number of second independent variable steps used. This is needed next time the EAP routine is called so that the old results table can be cleanly deleted.
134		{EditGoto EAP:A1}	Goto the "new" EAP plot and finish.
135			
136	series_chng	{calc}{SETOBJECTPROPERTY +"EAP:G$Series["&@STRING(loop1_count,0)&",1].Marker_Style",+marker_style}	This gives each series a unique marker style.
137			

	A	B	C
138	series_fill	{Series.Data_Range loop1_count, +"EAP:B"&@STRING(+31+loop1_count,0)&"..EAP:"&@CHAR(col_number-1)&@STRING(+31+loop1_count,0),1}	This fills each series with data from the results table.
139			
140			
141	loop2_calc	{LET $tscope_d,loop1_count}	
142		{LET +"EAP:"&@CHAR(col_number)&"31",loop1_count}	
143		{IF eap_option=1}{FOR loop2_count,eapvar_min,eapvar_max,eapvar_step,eap_calc_angle}	
144		{IF eap_option=0}{FOR loop2_count,0,eapvar_nstep,1,eap_calc_beta}	
145		{LET col_number,col_number+1}	
146		{LET row_number,32}	
147			
148	setup_varyangle	{SETOBJECTPROPERTY "loop-props:eapvarname.Label_Text", "Mis-alignment Angle"}	This routine is run to set up the loop parameters dialog box for varying the misalignment angle.
149		{SETOBJECTPROPERTY "loop-props:eapmintext.Label_Text", "Mini-mum (μrad)"}	The labels for the input boxes are changed to reflect the required parameters.
150		{SETOBJECTPROPERTY "loop-props:eapmaxtext.Label_Text", "Maxi-mum (μrad)"}	
151		{SETOBJECTPROPERTY "loop-props:eapsteptext.Label_Text", "No. of steps"}	
152		{LET $EAP:$D$25, +"Backscatter value of"}	This sets up the "Backscatter value of 'value' /(m-sr). line below the EAP plot.

	A	B	C
153		{LET $EAP:$F$25, +$beta}	
154		{LET $EAP:$G$25, +"/(m-sr)."}	
155		{LET $EAP:$I$14, +"misalignment"}	This sets up the correct label for the symbols and lines used for the second independent variable.
156		{LET $EAP:$I$15, +"angle (μrad)."}	
157		{SETOBJECTPROPERTY "$EAP:$I$14.Alignment", "Center"}	This ensures text alignment is correct.
158		{SETOBJECTPROPERTY "$EAP:$I$15.Alignment", "Center"}	As this is the last line in the subroutine execution of the main macro routine resumes.
159			
160	eap_calc_angle	{LET $align_angle, +loop2_count}	This routine is used when misalignment angle is the second independent variable. It sets up and runs the solver to determine the pulse energy required for a given misalignment angle and telescope diameter.
161		{LET $NRG, Guess}{solver}	Set energy to a small value. Call the solver routine.
162		{IF col_number=66}{LET +"EAP:A"&@STRING(row_number,0), $align_angle}	This is one of the routines that creates the results table. If this is the first loop over the alignment angle write the misalignment angle in column A.
163		{LET +"EAP:"&@CHAR(col_number)&@STRING(row_number,0),$NRG}	Write the solved value of the energy into the results table.
164		{LET row_number,row_number+1}	Increment the row (misalignment angle) loop and return to the routine from which this one was called.
165			
166	setup_varybeta	{SETOBJECTPROPERTY "loop-props:eapvarname.Label_Text", "Back-scatter"}	This routine sets up the labels on the input parameter dialog box for varying back-scatter.

	A	B	C
167		{SETOBJECTPROPERTY "loop-props:eapmintext.Label_Text", "Mini-mum /(m-sr)"}	
168		{SETOBJECTPROPERTY "loop-props:eapmaxtext.Label_Text", "Maxi-mum /(m-sr)"}	
169		{SETOBJECTPROPERTY "loop-props:eapsteptext.Label_Text", "No. of steps"}	
170		{LET $EAP:$D$25, +"Misalignment angle is"}	This sets up the line below the plot that indicates the value of misalignment used.
171		{LET $EAP:$F$25, +$align_angle}	
172		{LET $EAP:$G$25, +"μrad."}	
173		{LET $EAP:$I$14, +"backscatter"}	This modifies the label on the right of the plot to correctly indicate that backscatter is the second independent variable.
174		{LET $EAP:$I$15, +"(/m-sr)."}	
175		{SETOBJECTPROPERTY "$EAP:$I$14.Alignment", "Center"}	Make sure label alignment is correct.
176		{SETOBJECTPROPERTY "$EAP:$I$15.Alignment", "Center"}	Return to main routine.
177			
178	eap_calc_beta	{LET $beta, +10^(a+bval*loop2_count)}	This routine is called when backscatter is the second independent variable. This selects an intermediate values of back-scatter such that values are uniformly dis-tributed along a log axis.
179		{LET $NRG, Guess}{solver}	Set energy to a small value and call the solve routine.
180		{IF col_number=66}{LET +"EAP:A"&@STRING(row_number,0), $beta}	If this is the first loop over the range of backscatter values write the backscatter value into the first column of the results table.

	A	B	C
181		{LET +"EAP:"&@CHAR(col_number)&@STRING(row_number,0),$NRG}	Write the solved energy value into the results table.
182		{LET row_number,row_number+1}	Increment the row counter and return.
183			
184	solver	{Optimizer.Reset}{Optimizer.Solution_cell $PBAD}	This routine solves for the energy required. Set OPTIMIZER to solve for Pbad.
185		{Optimizer.Solution_goal "Target Value:"}	Set up as target value for Pbad.
186		{Optimizer.Target_Value 0.5}	We want Pbad=0.5 (=Pgood).
187		{Optimizer.Variable_cells $NRG}	We want to vary the energy.
188		{Optimizer.Solve}	Solve! Then return to calling routine.

Appendix (Id) The expanded MLE lookup table

Omega	M	b0	alpha	gamma	chi	g0	epsilon	delta	mu
0.2	10	5.6309	1.0665	1.4795	2.7988	63020	0.20249	9.4704	0.37968
0.2	20	7.0191	1.0952	1.4894	28.861	7.0698E-09	0.19923	0.80261	-0.0033124
0.2	30	6.9391	1.1591	1.3591	26.675	2.1075E-09	0.27401	0.53508	-0.051404
0.2	40	6.9859	1.3591	1.2936	70.699	4.1211E-11	0.25447	0.6538	0.050179
0.5	10	9.8489	1.052	2.6339	0.87423	3.6238	1.6357	0.23823	0.21661
0.5	20	10.406	1.1243	2.3859	0.89227	5.4419	0.96304	0.49395	0.23701
0.5	30	9.7439	1.1989	2.0932	0.92911	15.715	0.64088	1.1235	0.27069
0.5	40	11.216	1.2045	2.2094	0.91983	14.998	0.61835	1.0877	0.26377
0.5	50	12.718	1.2105	2.4001	0.88382	4.2306	1.0154	0.38244	0.2063
1	10	13.999	1.0783	4.1771	0.85915	3.8397	1.749	0.27177	0.17588
1	20	17.703	1.1106	4.1842	0.85994	4.8469	1.2675	0.43126	0.1894
1	30	17.949	1.1753	3.9817	0.88534	5.4245	1.0363	0.54923	0.18741
1	40	16.409	1.2258	3.5127	0.9059	4.4983	1.0058	0.52317	0.18236
2	20	641.07	1.0434	150.06	0.87606	5.2751	1.4394	0.42963	0.14629
2	30	52.948	1.1306	11.926	0.87923	4.5601	1.5913	0.35639	0.13586
2	40	48.04	1.153	10.215	0.88359	5.623	1.3207	0.48144	0.14588
3	20	4.6308	1.1923	1.2535	0.9145	6.2318	1.3798	0.5307	0.1462
3	25	6.6127	1.1843	1.573	0.887	4.3866	2.2939	0.2345	0.1082
3	30	9.6148	1.18	2.0453	0.9001	3.5357	3.1954	0.1401	0.0807
3	35	13.067	1.1495	2.5687	0.8758	4.2848	2.5322	0.2026	0.1
3	40	14.003	1.1862	2.7099	0.8854	3.5066	4.0879	0.1054	0.0761
4	20	7.4777	1.136	1.4958	0.77911	7.5634	1.2927	0.68357	0.21171
4	30	293.11	1.0632	62.546	0.89954	6.5971	1.5163	0.46486	0.11711
4	40	2707	1.0894	680.86	0.91805	5.9809	1.6426	0.40951	0.111
6	30	16.62	1.0927	2.6333	0.84545	10.418	1.1726	0.82424	0.17307
6	40	16.62	1.0927	2.6333	0.84545	10.418	1.1726	0.82424	0.17307
6.7	20	0.2318	4.0951	0.0196	0.2138	17.454	1.1469	0.8738	0.4349
6.7	25	0.7783	5.6302	0.0499	0.5362	19.252	0.9637	1.2103	0.3021

6.7	30	2.2702	1.5914	0.4216	0.7402	12.063	1.1882	0.8432	0.2037
6.7	35	5.7615	1.1484	1.1356	0.8928	9.3993	1.2744	0.708	0.1468
6.7	40	9.832	1.0981	1.8154	0.9536	7.7512	1.4531	0.544	0.1122

Appendix II

Direct global measurements of tropospheric winds employing a simplified coherent laser radar using fully scalable technology and technique

Michael J. Kavaya

NASA/Marshall Space Flight Center, Code EB54, Huntsville, AL 35812 USA
michael@lidar.msfc.nasa.gov

Gary D. Spiers

Center for Applied Optics, University of Alabama, Huntsville, AL 35899 USA
garys@photon.msfc.nasa.gov

Elena S. Lobl

Hughes STX, 620 Discovery Drive, Huntsville, AL 35806 USA

Jeff Rothermel

NASA/Marshall Space Flight Center, Code ES43, Huntsville, AL 35812 USA
jeff@pcjxr.msfc.nasa.gov

Vernon W. Keller

NASA/Marshall Space Flight Center, Code PS02, Huntsville, AL 35812 USA

ABSTRACT

Innovative designs of a space-based laser remote sensing "wind machine" are presented. These designs seek compatibility with the traditionally conflicting constraints of high scientific value and low total mission cost. Mission cost is reduced by moving to smaller, lighter, more off-the-shelf instrument designs which can be accommodated on smaller launch vehicles.

Paper 2214-31, SPIE's International Symposium on Optical Engineering in Aerospace Sensing, Technical Conference 2214 on Space Instrumentation and Dual-Use Technologies, session on "Faster, Cheaper, Smaller Space Science Optical Instruments," Orlando, FL (6 April 1994).

1. INTRODUCTION

Measurements of tropospheric winds from space are highly desired for many NASA, NOAA, DOD, DOE, EPA, and commercial applications.[1,2] These include global climate change research, improved weather forecast accuracy, optimum aircraft routing for passenger safety/comfort and for fuel/time savings, commercial shipping storm avoidance, pollution research and regulation enforcement, and military planning. Improved weather forecasting will save lives lost to storms, as well as reduce the number of false alarms. Numerous studies have indicated that the optimum measurement approach for winds from space is a pulsed coherent laser radar (CLR)[3-5]. NASA recently completed dual Phase A and B studies, by GE Astro Space[6] and Lockheed[7], for a full tropospheric profiling instrument named the Laser Atmospheric Wind Sounder (LAWS). The studies both recommended a pulsed CO_2 laser CLR system with pulse energy near 20 J, pulse repetition frequency (PRF) near 5 Hz, optical diameter near 1.6 m, and full-time operation (100% orbit duty cycle). However, the projected mission costs were deemed unacceptable for this new era of reduced NASA resources, and the projected spacecraft resource requirements exceeded the capabilities of small satellites. NASA's Marshall Space Flight Center (MSFC) has therefore conducted an in-house effort to investigate innovative versions of LAWS which are smaller, lighter, less expensive; which consume less power, require less heat removal, fit on small spacecraft and launch vehicles; which provide valuable engineering data and space heritage; and which still deliver significant science product consistent with NASA's Mission To Planet Earth (MTPE). The working name for these instruments is Autonomous Earth Orbiting Lidar Utility Sensor (AEOLUS), after the mythical Greek god of wind. This paper reports on the progress to date of this in-house effort.

2. WHAT IS AEOLUS?

The AEOLUS project is a series of point designs of a small, lightweight, low cost, low risk instrument for measuring winds from space in regions of high aerosol backscatter. The mission goals are to:

1) provide valuable scientific information in support of NASA's MTPE,
2) demonstrate space operation of key technologies required for a full-scale LAWS,
3) implement a logical, affordable evolutionary process leading to a full-scale LAWS measurement of global tropospheric winds.

The ground rules we followed are:

1) to use components that are as close to "commercial off the shelf (COTS)" as possible,
2) to use technology and a measurement technique that is capable of scaling up to make the full-scale LAWS measurement,
3) to design a flexible instrument capable of being accommodated on a variety of platforms in space such as small satellites, the space shuttle, and space station.

The instrument design process we followed is shown in Figure 1.

3. MEASUREMENT TECHNIQUE

Both the choice of a measurement technique for AEOLUS and subsequent consideration of design trade-offs within the chosen technique have confirmed that measurement of wind from space is a complex undertaking that contains numerous and sometimes subtle interactions between:

1) the laser radar instrument parameters,
2) the available laser radar technology,
3) the capabilities of the instrument bus or carrier,
4) the launch vehicle, and
5) the atmospheric target and its assumed properties.

When the various requirements of the mission that must be achieved simultaneously are considered from a system perspective, the sensor of choice for this mission is a pulsed CLR. These joint requirements include:

1) horizontal wind measurement accuracy of about 1 m/s or better,
2) sufficiently large cross-track measurement swath width for areal coverage,

3) minimal horizontal wind measurement bias,
4) horizontal wind measurement resolution of about 100 km or smaller,
5) best possible vertical resolution,
6) maximum possible allowed horizontal wind magnitude,
7) minimal prime power, cooling, and downlink data rate requirements,
8) minimal instrument mass and volume,
9) maximum mission duration,
10) eyesafe fluence exposure,
11) low mission cost.

Requirement 1 leads to the need for nearly collocated, biperspective line of sight (LOS) wind measurements. Because of spatial variability in the horizontal wind field, many LOS measurements are needed in each areal resolution element (e.g., 100 km x 100 km square) in order to reduce the contribution to error from undersampling. Since the point on the earth directly below the spacecraft moves at 7.3 km/s (350 km orbit height), the 100 km resolution requirement means that the time available for an accurate LOS horizontal wind measurement in a 100 km square is only about 14 s divided by the number of 100 km squares being probed in the cross-track direction. Using our current number of 4 cross-track squares yields about 3.5 s for each horizontal wind measurement. (The full-scale LAWS had 10 cross-track squares.) Requirement 2 means the laser beam must be scanned. The scanning may be continuous or step-stare. Continuous-scanning is preferred by the spacecraft designer who must compensate the angular momentum. Since continuous scanning involves changing the beam pointing direction with time, an accurate LOS wind measurement must occur over a short time interval due to both the varying spacecraft-earth relative velocity along the LOS, and due to the varying probe direction of the laser beam in the wind. Thus the number of laser shots per LOS measurement divided by the laser PRF must be small. Pulsed CLR satisfies this by making a measurement with as few laser shots as one. By comparison, techniques that employ many laser shots per LOS measurement, such as pulsed noncoherent laser radar (NLR), must use a high laser PRF. A higher PRF increases the required laser lifetime (in pulses), increases the on-board data processing rate, and increases the data downlink rate unless on-board combining of multiple laser shot data is performed. This is true even if the total transmitted pulse energy per LOS wind measurement is the same as CLR. To date, however, NLR measurements have proven less photon efficient than CLR, and more total energy per LOS measurement must be transmitted. The important comparisons of prime power and cooling require knowledge of each laser's efficiency. Some methods of combining laser shot data on board increase the risk of velocity bias, and preclude data processing improvements on the ground.

4. COMPONENTS OF A SPACE-BASED CLR

It was stated above that the system designer must account for the interactions of the CLR instrument, the atmospheric or earth surface target of interest, the launch vehicle, and the carrier or bus connecting the instrument to the launch vehicle. Each of these items has levels of further subdivision. A CLR broadly consists of a laser transmitter, an optics subsystem, a receiver, a control computer, a data acquisition subsystem, and a data processing computer. A simplified schematic of a CLR is shown in Figure 2. The laser subsystem consists of an optical pulse generating unit and one or two continuous-wave (CW) lasers to perform the functions of master oscillator and local oscillator (LO). The optics consist of lenses, mirrors, beamsplitters, the beam expanding telescope, the beam scanner, and, if needed, a lag angle compensation (LAC) element. The receiver comprises an optical detector, and optics to combine the received photons from the atmosphere with the LO optical field. This combination must strive to match the shape, direction, curvature, and polarization of the LO field with the expected value of signal field.

5. SPACECRAFT AND LAUNCH VEHICLE ACCOMMODATION

The payload of the launch vehicle (i.e., spacecraft) consists of the carrier or bus mated to the scientific instrument(s). This payload must be accommodated by the launch vehicle in the categories of mass, volume, orbit height, orbit inclination, survivable launch vibration frequencies and amplitudes, and survivable launch accelerations. The cost of the launch vehicle and carrier must both fit in the mission budget. We are considering Pegasus XL, Conestoga, LLV, and Taurus class launch vehicles. The carrier must accommodate the needs of the instrument including electrical power, heat removal (thermal), orbit height, orbit inclination, electrical power storage in batteries, mass, data downlink rate, mechanical mating, pointing control and stability, etc.

A sun-synchronous orbit is preferred from the electrical power and heat removal viewpoints. The measurements occur over all latitudes and over all the earth after a few days. By contrast an equatorial orbit does not measure the higher latitudes, but

gives more coverage of low latitudes. It receives the launch advantage of the earth's rotation, but is less desirable for electrical power and heat removal.

Lower orbit heights allow a greater payload mass, but some of this mass gain is consumed by propellent needed for additional reboosts due to increased atmospheric drag. Lower heights also provide greater SNR for fixed nadir angle, but not necessarily for fixed cross-track coverage. Atmospheric drag also depends on the sunspot cycle, which will peak from 1999 to 2004. The designs described later assume a 350 km orbit height with a 30° nadir angle which yields a 400-km wide coverage centered below the spacecraft.

The data rate is proportional to the laser PRF, the number of desired range gates (the height resolution and coverage), and the fraction of each orbit spent taking data (orbit duty cycle). The data rate may be lowered by processing data on board before transmission. Maximum science is achieved by 100% orbit duty cycle. Downlinking all data allows research into optimum velocity estimation algorithms.

Assuming a suitably located ground station with a large (~5 m) diameter S-band antenna, data can be downlinked directly from the spacecraft to the ground station at a peak data rate of ~2 Mbit/s, but only during the time the spacecraft has LOS visibility to the receiving station. This available time on any given orbit varies from zero to >5 min. with a gap between downlink opportunities sometimes as long as 20 hrs. Thus on-board data storage of several hundred Mbit may be required. A typical ground station with a small (~1 m) diameter antenna will handle only a few 10's of kbit/s. This would require use of several ground stations. At greater cost, data could be downlinked through an S-band omnidirectional antenna to the 26-m ground antenna network of the Deep Space Network (DSN), or via a geostationary communications satellite such as the Tracking and Data Relay Satellite System (TDRSS).

6. PULSED CLR DESIGN TRADES

Choosing a design point for a pulsed CLR to measure winds from space leads one to work in an onerous multi-dimensional space consisting of a dimension for each parameter of the CLR instrument, the atmospheric target, the carrier capabilities, and the launch vehicle capabilities. All of these parameters are interconnected and must be dealt with. Some of these interconnections have been previously discussed.[8] Varying one parameter to solve one problem often produces one or more new problems. Often a mean value description is inadequate and a parameter's probability distribution function (PDF) must be used (e.g., aerosol backscatter). Possible correlations among parameters must also be considered (e.g., aerosol backscatter vs. wind turbulence vs. wind shear). Some design choices are continuous (e.g., laser pulse energy, optical diameter), while others are discrete (e.g., velocity calibration with or without an earth surface return, conical scanning with a rotating telescope or a rotating wedge or a rotating flat mirror, active or passive heat removal).

An illustrative example of a design trade is the choice of design nadir angle θ, the angle between the nadir direction and the LOS laser beam direction, for a laser beam conically scanning about nadir. (All our designs assume a constant nadir angle. A variable nadir angle would increase complexity, risk, cost, and mass.) Many aspects of the system design depend on nadir angle. In some cases the dependence on nadir angle can be easily pictured, while in other cases the dependence is complex, and should be modeled on a computer. Table 1 summarizes some of the simple cases. We assume for the moment a flat earth, and do not distinguish between the nadir angle as the photons leave the CLR in space, and their nadir angle in the atmosphere. This assumption becomes more seriously incorrect as the nadir angle increases. Seeking first to maximize signal-to-noise ratio (SNR) (see case 1 in Table 1), we consider that the signal power falls inversely as the square of the slant range R. The flat earth slant range varies as $1/\cos\theta$. The noise power is proportional to the detection or search bandwidth B_S, which equals $(2/\lambda)V_S$, where V_S is the velocity search bandwidth. For a maximum design horizontal wind in any direction, V_{HM}, we find $B_S = (2/\lambda)(2V_{HM})\sin\theta$. The total SNR function is therefore $(\cos^2\theta)/\sin\theta$. The nonintuitive optimum nadir angle appears to be 0°, or straight down. However, it has been shown that SNR is not a good figure of merit (FOM) for wind velocity measurements. Picturing the detected signal in the frequency domain, the signal power is gathered in just a few, or even one, frequency bins, while the noise power, assumed white, is spread across all frequency bins. A better FOM is the ratio of the signal height to the level of the "grassy" noise, i.e., the ratio of the total average signal energy in the observation time to the spectral density level of the noise[3,9]. This parameter Φ = SNR x M, where M is the number of data samples used to make the frequency estimate[9]. The number of data samples per estimate is proportional to

both the sampling frequency of the data recorder and the observation time for one estimate. Holding the desired height resolution of the measurement constant means that the observation time goes as $1/\cos\theta$. Holding V_{HM} constant, and sampling the data stream fast enough to avoid frequency aliasing causes the sampling frequency to go as $\sin\theta$. This is case 2 in Table 1 and again yields an optimum nadir angle of 0°, but with a weaker function of θ. Next we consider that the mission goal is horizontal wind measurements and not just LOS measurements. The alignment of each LOS measurement with the horizontal wind goes as $\sin\theta$ and is shown in case 3 of Table 1. The optimum nadir angle is now 45°. This combination of LOS velocity estimation performance with horizontal alignment is heuristic and not rigorous. Two techniques of effecting a conical scan about nadir are a rotating telescope and a rotating wedge. If a wedge is used to deflect the laser beam by θ, the CLR optical diameter is reduced by the factor $\cos\theta$. This effect is added in case 4, where we specifically assume that atmospheric refractive turbulence effects are small, and that there is no transmitter/delayed back-propagated local oscillator (BPLO) misalignment angle α. The angle α occurs between the transmitted laser pulse direction and the direction of the imaginary BPLO beam as the backscattered photons reenter the CLR. The optimum nadir angle becomes 35°. We may also heuristically add the goal of large cross-track coverage by the satellite sensor. For a flat earth, we multiply by $\tan\theta$. This is included in case 5. The optimum angle becomes 55°. Case 6 assumes a rotating telescope, removes the wedge scanner, and yields that larger nadir angles are always better. We do not use the FOMs in cases 5 and 6 since the treatment of swath width is so arbitrary. Our computer simulation for estimating the performance of candidate mission designs uses a spherical earth, and also includes the more complex effects of atmospheric extinction, atmospheric refractive turbulence, and misalignment angle. Using our more sophisticated simulation for cases 4 and 5 produces the smaller optimum angles of 33° and 47°, respectively (see Figure 3). It is reasonable that addition of extinction and a spherical earth would favor smaller nadir angles. The simulation parameters correspond to our point design 5, which is discussed below. Note that we used a constant misalignment angle of 7.3 μrad, which causes a budgeted 3 dB misalignment loss at our nominal nadir angle of 30°, but varying loss at other nadir angles.

Future refinements to our FOM for just the nadir angle design trade might include the effects of nadir angle on aerosol backscatter, land backscatter, ocean backscatter, and the probability of intercepting clouds. Also related are the cost and mass of the wedge, and the effects on atmospheric shot spacing of wedge rotation rate and laser PRF.

Table 3: Selection Of Design Nadir Angle

Case	SNR $(\cos^2\theta)/\sin\theta$	Number Data Samples $\tan\theta$	Horizontal Alignment $\sin\theta$	Wedge Scanner $\cos\theta$	Cross-Track Width $\tan\theta$	Total Function	Optimum Nadir Angle (deg.)
1	4					$(\cos^2\theta)/\sin\theta$	0
2	4	4				$\cos\theta$	0
3	4	4	4			$\cos\theta\sin\theta$	45
4	4	4	4	4		$(\cos^2\theta)\sin\theta$	35
5	4	4	4	4	4	$(\sin^2\theta)\cos\theta$	55
6	4	4	4		4	$\sin^2\theta$	90

The misalignment angle α is another important design trade issue, especially when selecting the laser wavelength of the CLR[8], or when selecting the optical diameter. Frehlich[10] has examined the effect of misalignment angle α on degradation of the CLR heterodyne or mixing efficiency, η_{MIX}; which is important since both SNR and Φ are proportional to it. We employ Frehlich's exact results for a circular optical aperture of diameter D, a Gaussian transmitted beam with diameter optimally matched to D, a monostatic CLR, far field operation, and negligible refractive turbulence effects. For degradations less than 15 dB, the points approximately follow $\eta_{MIX} = 0.42 \exp[-(q/2.8)^2]$, where $q = (\pi D\alpha/\lambda)$. This is a strong function of the ratio q, which includes optical diameter, misalignment angle, and optical wavelength. If a wedge scanner is used, the diameter D refers to the smaller value

exiting the wedge. For a fixed budgeted loss in SNR due to misalignment, the ratio q must be held constant. Smaller values of λ require proportionally smaller values of allowed misalignment. This is shown in Figure 4 for two wavelengths and the parameters of our point design 5. When $\alpha = 0$ and effects of refractive turbulence are negligible, the common intuition that larger values of D yield better performance is correct since SNR is proportional to receiver area = $\pi D^2/4$. However, nonzero values of α cause a reduction in this quadratic gain of performance with increasing D, and may even cause an absolute reduction in performance. This is shown in Figure 5 using the parameters of our point design 5. Even without the misalignment effect, thus having the promise of quadratic gain in performance, the optical diameter would be limited due to the penalties of mass, volume, cost, need for high optical quality, and the need to conically scan the beam. Misalignment even further reduces the optimum design diameter. We are attempting to merge the behavior of the CLR with information about realistic on-orbit misalignment angles. The actual misalignment angle will consist of contributions from prelaunch assembly and alignment of the optical subsystem, further misalignment from launch stress and orbit life, laser shot pointing jitter, and spacecraft pointing jitter during the round trip time of the transmitted photons (~ 3 ms). Techniques to eliminate the first three contributors are possible, but they complicate the instrument design.

7. INSTRUMENT DESIGNS

The NASA/MSFC AEOLUS team has nearly completed five instrument point designs. We are carrying two candidate laser technologies, the CO_2 laser at 9.11 μm wavelength, and the Tm,Ho:YLF diode-pumped solid-state laser at 2.06 μm. From our nearly COTS ground rule, and our desire for smallsat capability, we have permitted maximum laser pulse energies of 400 and 200 mJ, respectively, and a maximum optical diameter of 50 cm. Each design is examined from the mechanical, electrical, thermal, optical, laser, CLR wind measurement performance, and spacecraft accommodation perspectives. An example of CLR performance prediction for our point design number 5 is shown in Figure 6. Five curves are plotted against the atmospheric aerosol backscatter coefficient. The reflectances of land and water may also be converted into these backscatter units. This description permits scientists to determine the applicability of each CLR to measure winds of various atmospheric targets such as clear air, clouds, dust, boundary layer air, jet streams, etc. From top to bottom, the five curves are SNR_M, the unrealistic limiting case of matched filter SNR, SNR_S, the more realistic SNR calculated from the noise admitted into the velocity search bandwidth, Φ, as discussed earlier, P_g, the probability that a LOS wind estimate is "good", and σ_V, the standard deviation or spread of the "good" wind estimates[9]. The "good" wind estimates are clustered around the true value of the wind speed, while the "bad" estimates are uniformly distributed over a region of width V_S. All the values of σ_V are sufficiently small to provide excellent performance. Even as P_g falls to 20% for low values of backscatter, σ_V remains smaller than 0.4 m/s. Therefore, the key performance criterion to monitor is P_g. Since the backscatter value that yields $P_g = 0.5$ occurs near $\beta(2.06\ \mu m) = 2.5 \times 10^{-6}\ m^{-1}sr^{-1}$, we refer to that number as the aerosol backscatter sensitivity of design 5. As can be seen, lower values of $\beta(2.06\ \mu m)$ will produce fewer but usable velocity estimates. Note that for $\beta(2.06\ \mu m) = 2.5 \times 10^{-6}\ m^{-1}sr^{-1}$, SNR_M ~ 3 dB, SNR_S ~ -15 dB, $\Phi \sim 6$, and σ_V ~ 0.3 m/s.

All five of our point designs are contrasted in Table 2. The top row shows the backscatter sensitivity of each design. Care must be taken when comparing these values at different optical wavelengths, since backscatter varies with wavelength. Common to all 5 designs are an SNR margin of 3 dB, a budgeted misalignment loss of 3 dB, a sun-synchronous orbit height of 350 km, a 30° nadir angle, a target altitude of 300 m, transmit and receive optics efficiencies of 0.9 each, and no polarization mismatch loss. Figure 7 contrasts the sizes of designs 1-5 with the Lockheed LAWS Phase B design[7]. Design 5 has a pulse energy-receiver aperture product 15 dB below designs 3-4 in order to be accommodated on a Pegasus rocket. It achieves considerable volume and mass savings. The orbit average electrical power needed by design 5 is higher than 3-4 due to the increase of orbit duty cycle to 30% (a factor of 6), and an increase in laser PRF to 50 Hz (a factor of 5). Designs 2,4, and 5 use a rotating wedge to create a conical scan about the nadir direction. Designs 1 and 3 have two fixed pointing directions, fore and aft, to allow biperspective wind measurements along a line parallel to the ground track, but offset by 144 km. The two views of a single point in the atmosphere would be accomplished by switching the CLR between two 50 cm telescopes, and would occur about 40 s apart. This configuration has less science value than the conical scan. Comparing the 9.11 μm designs 1-2 with the 2.06 μm designs 3-4, the cost of scanning in mass and power, as well as its lower volume can be seen.

No attempt has been made to have equal science value between the point designs at 2.06 and 9.11 μm. A study is underway to quantify the ratio of backscatter values between the two wavelengths for various candidate atmospheric targets within the

sensitivity range of our different point designs. Note also that holding the misalignment loss fixed at 3 dB causes the misalignment angle specification to become stricter at 2.06 μm. Our designs are not yet mature enough to quantify the effect this stricter specification might have on instrument mass, volume, complexity, and cost; or on the suitability of candidate spacecraft.

8. CONCLUSIONS

Global tropospheric wind measurements are highly desired and will provide many benefits. Numerous studies have selected coherent laser radar as the optimum technique. Atmospheric winds have been successfully measured with coherent laser radar since 1967. A full-scale mission which measures the lowest levels of aerosol backscatter is not practical in today's economic climate. However, significant scientific benefits are possible with a smaller and more affordable instrument. Significant benefit could result in only a few years by starting a faster, smaller, cheaper mission now. NASA/MSFC is ready to design and perform such a mission. The mission will provide exciting science and will also provide valuable information for a future full-scale effort.

9. ACKNOWLEDGMENTS

The AEOLUS project was conceived by J. W. Bilbro of NASA/MSFC. The authors appreciate the suggestions of R. G. Beranek, D. B. Bowdle, R. G. Frehlich, and R. J. Koczor; and the design work of F. Amzajerdian, J. A. Dunkin, R. Eng, J. C. Fikes, P. L. Hunt, J. Jackson, S. C. Johnson, J. W. Redmon, Jr., W. A. Till, and S. P. Tucker. One of us (GDS) gratefully acknowledges the support of Dr. Ramesh K. Kakar, NASA Headquarters, under contract NAS8-38609.

10. REFERENCES

1. W. E. Baker, "Why We Need LAWS," Storm, The World Weather Magazine 1(1), 26-30, 1993.
2. R. Sadourny, "Importance of global Doppler lidar wind profiles from space for climate and environment studies," paper TuA1, p. 91, Tech. Digest of the 7th Conference on Coherent Laser Radar Applications and Technology, Paris, France, 19-23 July 1993.
3. R. T. Menzies, "Doppler lidar atmospheric wind sensors: a comparative performance evaluation for global measurement applications from earth orbit," Appl. Opt. 25(15), 2546-2553, 1986.
4. "Laser Atmospheric Wind Sounder (LAWS) Earth Observing System Instrument Panel Report," Vol. IIg, National Aeronautics and Space Administration, R. J. Curran, Chairman, Jan. 1987.
5. R. G. Beranek et al, "Laser Atmospheric Wind Sounder (LAWS)," Proc. SPIE 1062, 234-248, 1989.
6. "Definition and Preliminary Design of the Laser Atmospheric Wind Sounder (LAWS)," Phase II Final Report, NASA Contract NAS8-37589, Volume I, Executive Summary and Volume II, Final Report, GE Astro Space, 9/30/92.
7. "Design Definition of the Laser Atmospheric Wind Sounder (LAWS)," Phase II Final Report, DR-20, NASA Contract NAS8-37590, Volume I, Executive Summary, June 1992, and Volume II, Final Report, November 1992, Lockheed Missiles & Space Company.
8. M. J. Kavaya, "Wavelength trade considerations for space-based coherent lidar measurement of winds," paper MD3, p. 78, Tech. Digest of the 7th Conference on Coherent Laser Radar Applications and Technology, Paris, France, 19-23 July 1993.
9. R. G. Frehlich and M. J. Yadlowsky, "Performance of Mean-Frequency Estimators for Doppler Radar/Lidar," to be published in J. Atmospheric and Oceanic Technology, 1994.
10. R. G. Frehlich, "Heterodyne efficiency for a coherent laser radar with diffuse or aerosol targets," submitted to J. Modern Optics, 1993.

DESIGN / PARAMETER	NO. 1	NO. 2	NO. 3	NO. 4	NO. 5A THIN CLOUDS	NO. 5B THICK CLOUDS
PERFORMANCE						
BACKSCATTER(/M-SR)@50%	8.2E-09	1.1E-08	5.7E-08	7.6E-08	2.5E-06	3.9E-05
SNR MARGIN, dB	3	3	3	3	3	3
VERTICAL RESOLUTION, M	1000	1000	1000	1000	1000	64
MAXIMUM HORIZONTAL WIND, M/S	30	30	30	30	50	50
INSTRUMENT						
LASER WAVELENGTH, µM	9.11	9.11	2.06	2.06	2.06	2.06
SCAN TYPE	dual-look	scan wedge	dual-look	scan wedge	scan wedge	scan wedge
PULSE ENERGY, mJ	400	400	200	200	25	25
PRF, Hz	20	20	10	10	50	50
TELESCOPE DIAMETER, M	0.5	0.5	0.5	0.5	0.25	0.25
MISALIGNMENT LOSS, dB	3	3	3	3	3	3
MISALIGNMENT ANGLE, µRAD	13.9	16.1	3.15	3.64	7.28	7.28
SIZE, M	1.22x1.24x1.33	1.22(D)x1.35	1.22x1.24x1.33	1.22(D)x1.35	0.73(D)x0.99	0.73(D)x0.99
Inches	48.0x48.8x52.4	48.0(D)x53.3	48.0x48.8x52.4	48.0(D)x53.3	28.8(D)x38.9	28.8(D)x38.9
VOLUME, M3	2	1.6	2	1.6	0.4	0.4
ft3	71	55.8	71	55.8	14.7	14.7
MASS, Kg	231	266	191	226	125	125
lbs	508	585	420	497	275	275
POWER, W (STBY/WARM-UP/OPER)	160/332/437	168/378/476	75/182/355	83/226/391	83/221/331	83/221/331
ORBIT DUTY CYCLE, %	5	5	5	5	30	30
ORBIT AVERAGE POWER, W	203	219	107	122	180	180

Table 2 AEOLUS designs intercomparison.

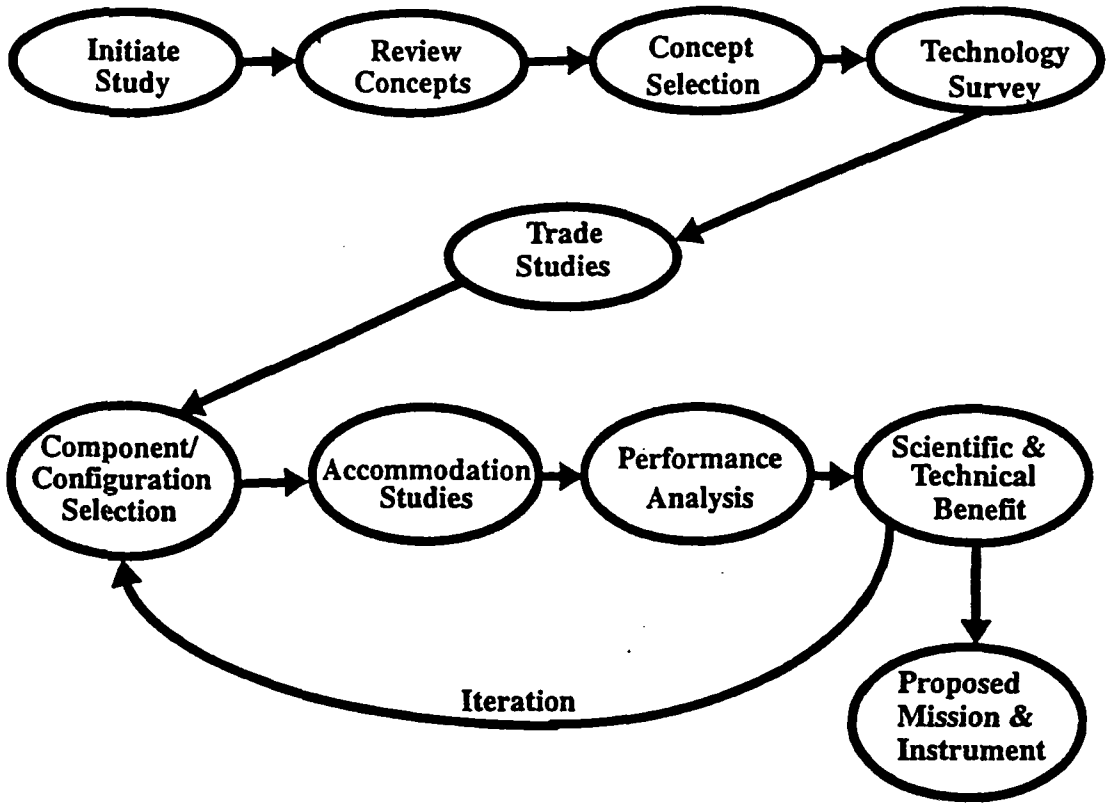

Figure 1 AEOLUS instrument design process.

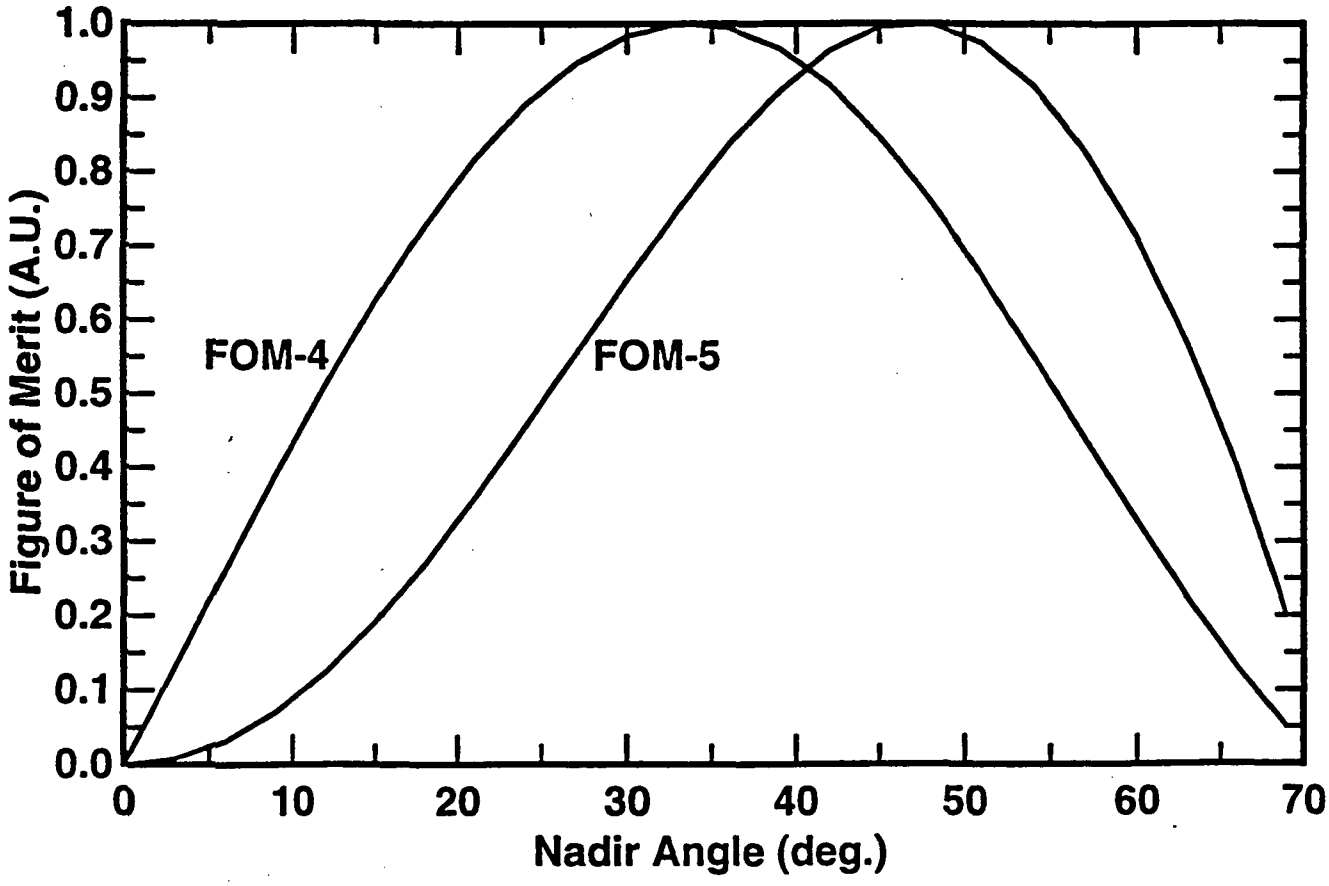

Figure 3 Two selected figures of merit as a function of nadir angle (see text).

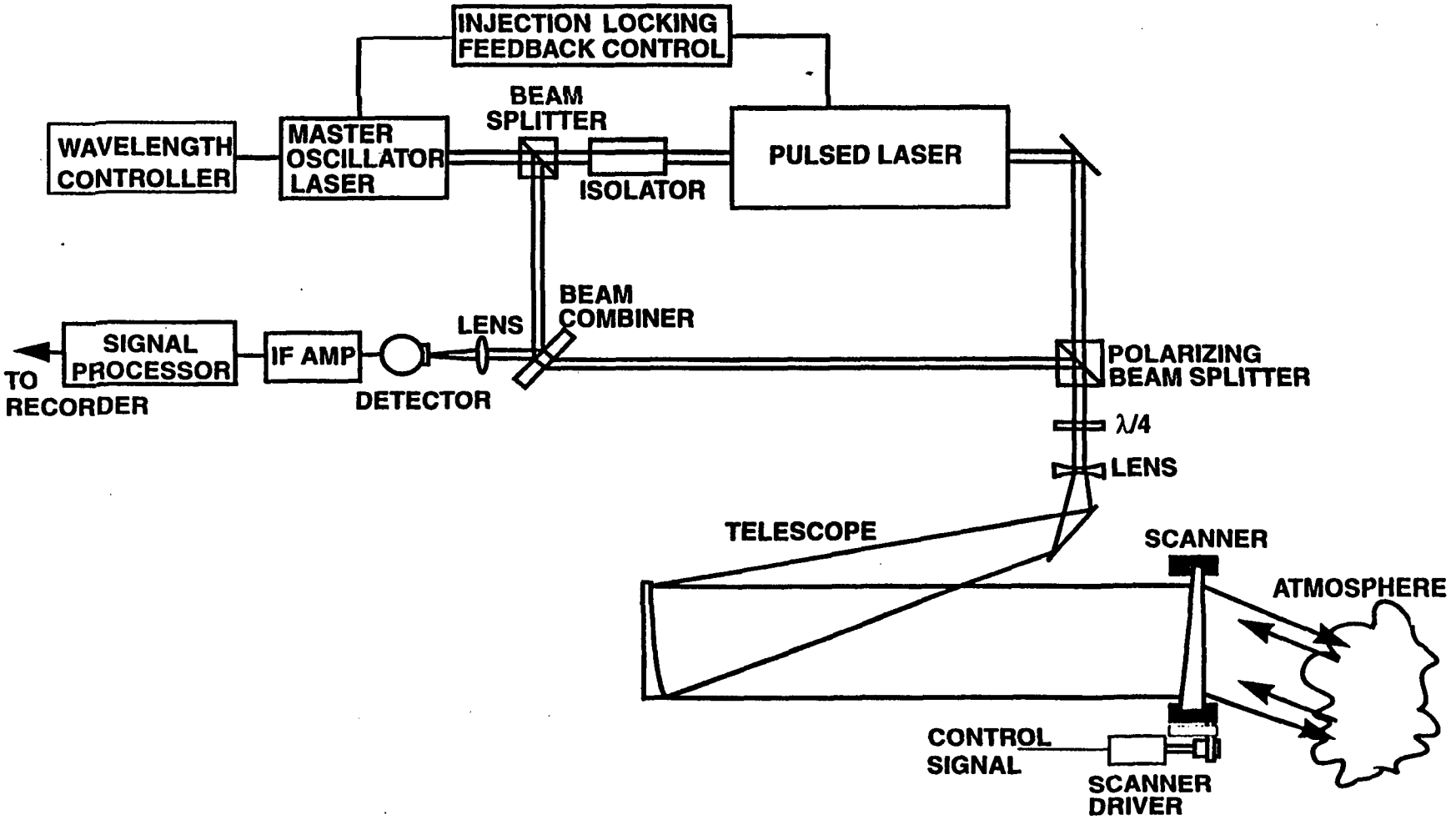

Figure 2 Optical Schematic for AEOLUS point design no. 5.

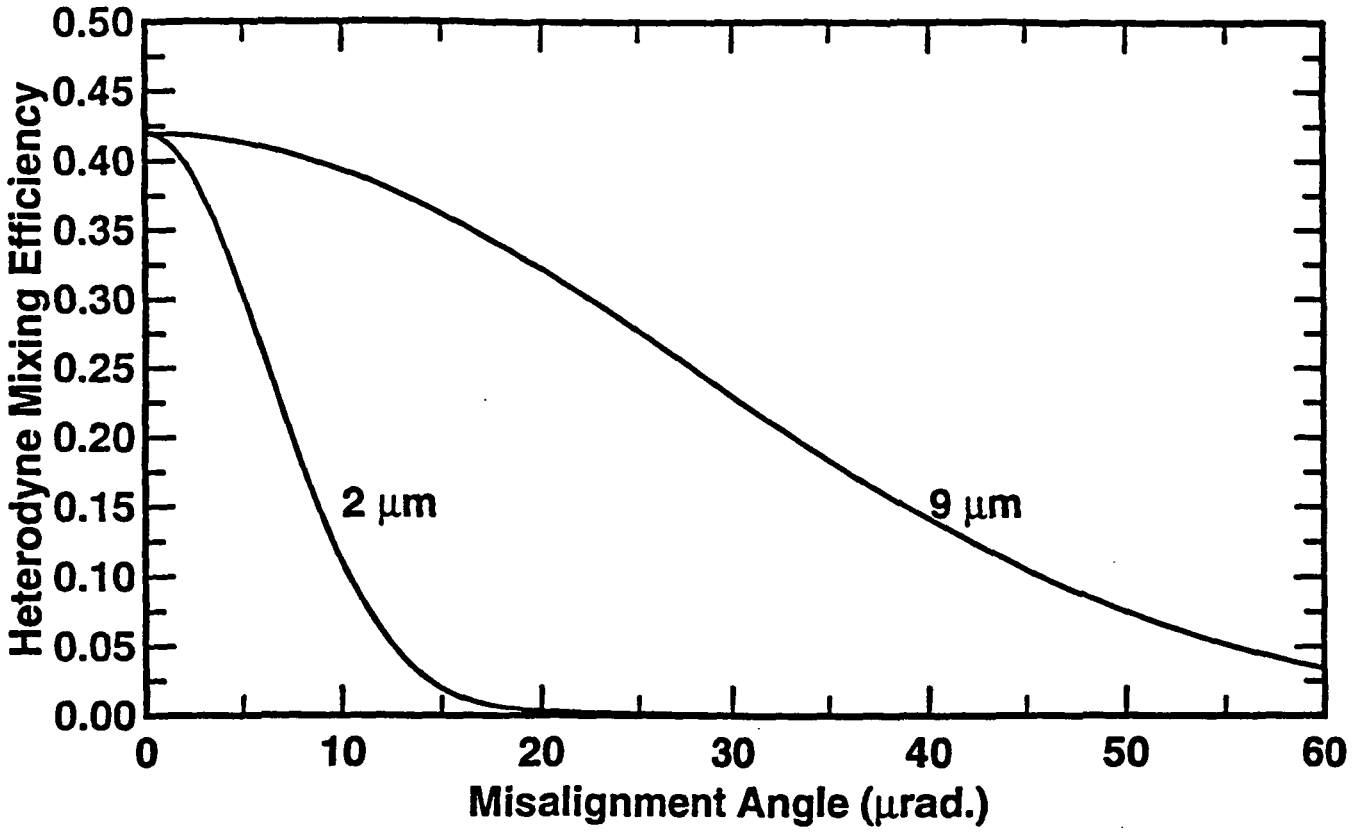

Figure 4 Heterodyne efficiency vs. misalignment angle for a 25 cm telescope, wedge scanner and 30 degree nadir angle.

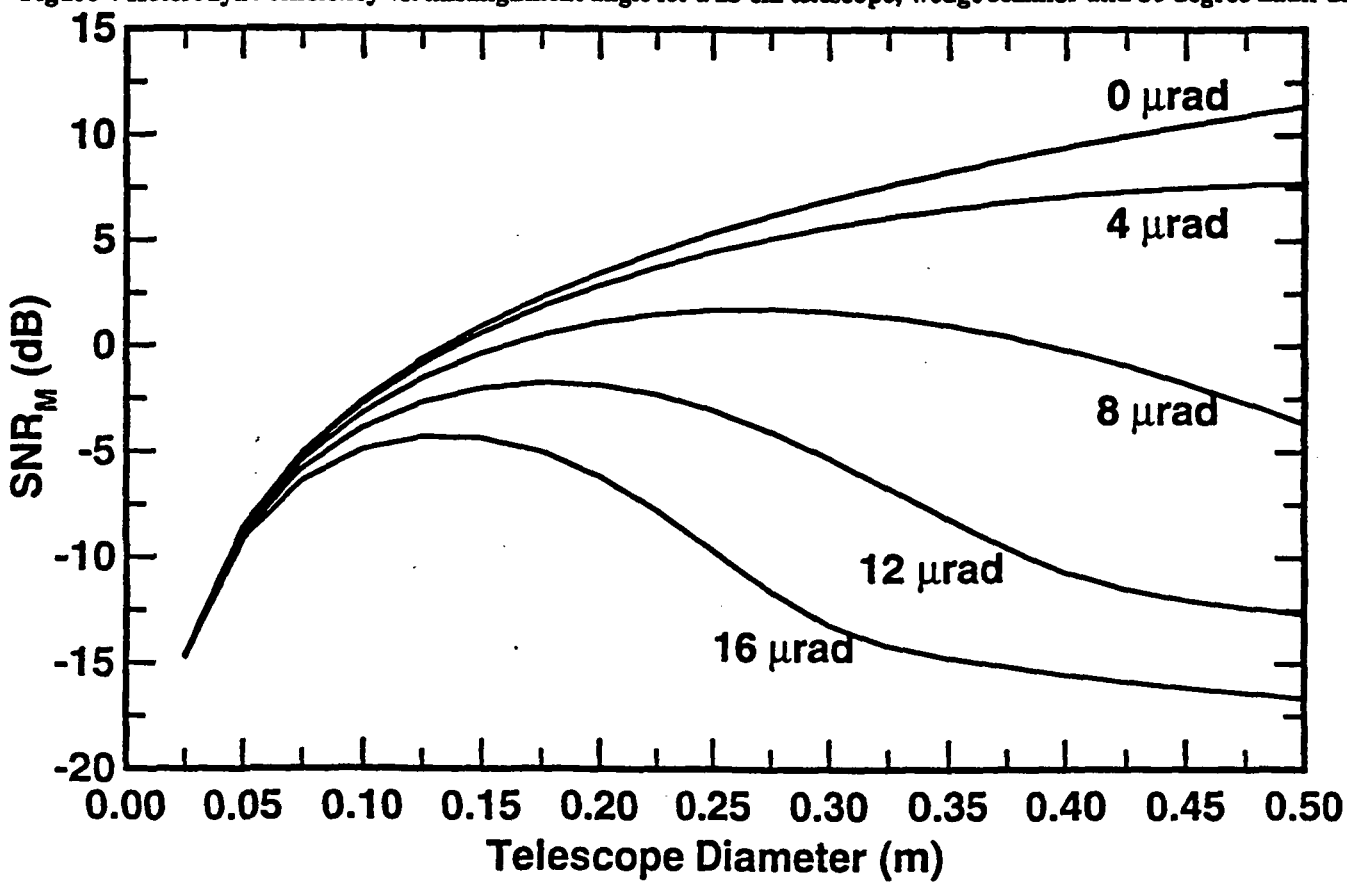

Figure 5 The variation of matched filter SNR with telescope diameter and misalignment angle for a wavelength of 2μm.

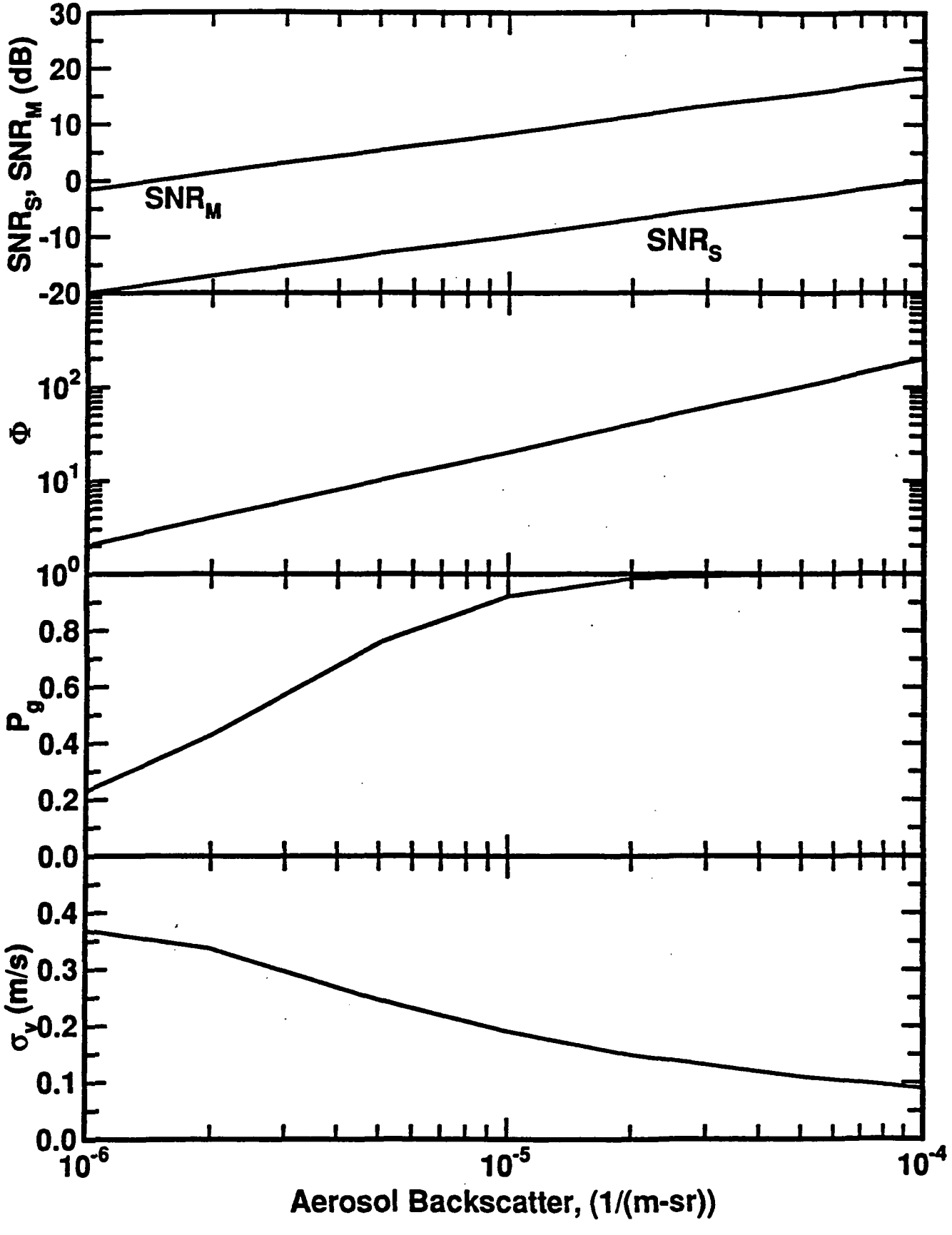

Figure 6 A representative performance analysis for Design No. 5 with a 1 km vertical integration range.

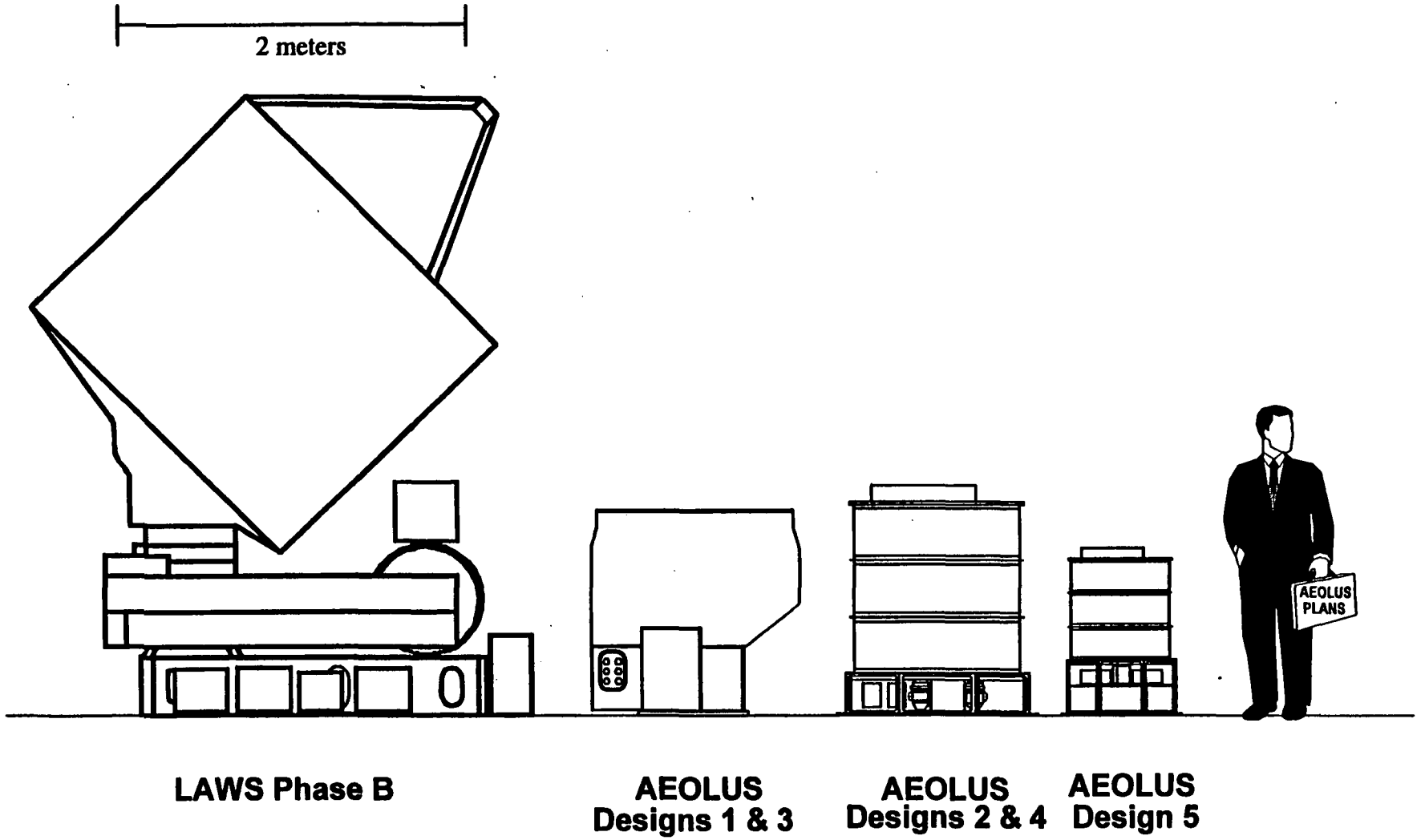

Figure 7 Comparison of AEOLUS designs and one of the LAWS Phase B designs.